Thermochimica Acta 510 (2010) 185–194

Contents lists available at ScienceDirect

Thermochimica Acta

journal homepage: www.elsevier.com/locate/tca

Thermal and morphological analysis of thermoplastic polyurethane–clay nanocomposites: Comparison of efficacy of dual modified laponite vs. commercial montmorillonites

Manas Mondal [a], Pijush K. Chattopadhyay [a], S. Chattopadhyay [a,*], Dipak Kumar Setua [b]

[a] Rubber Technology Centre, Indian Institute of Technology, Kharagpur 721302, India
[b] Defence Materials and Stores R and D Establishment, Kanpur 208103, India

ARTICLE INFO

Article history:
Received 3 May 2010
Received in revised form 8 July 2010
Accepted 9 July 2010
Available online 16 July 2010

Keywords:
Thermoplastic polyurethane
Nanocomposites
Laponite
Cloisite
Thermal analysis

ABSTRACT

Thermoplastic polyurethane (TPU)–clay nanocomposites were studied with respect to thermal properties and morphology. Different types of clay, e.g. modified laponite (ionic followed by covalent modification using different silanes) and montmorillonites (e.g. Cloisite 30B and Nanomer I.30E) were used. Activation energies (E) for thermal decomposition of nanocomposites were determined by Flynn and Wall technique. The changes in 'E' value with the level of conversion suggest a complicated degradation rate. Lifetime of composites was estimated by Toop's equation revealing higher lifetime for montmorillonite based composites. It was found that dual modification of laponite was sometimes more effective/equivalent to commercial montmorillonites regarding viscoelastic properties and thermo-dimensional stabilities of nanocomposites. Phase morphology, filler dispersion, RMS roughness obtained from SEM (including X-ray dot mapping), AFM analyses revealed the role of aggregates in degradation of properties of composites. Moreover, thermo-physical properties were dependent on the aspect ratio, polarity, and aggregation characteristics of clay into TPU.

1. Introduction

Thermoplastic polyurethane (TPU), especially the segmented TPU, has become popular for potential smart applications [1–3]. The development of 'TPU-nanocomposite' is another field fetching significant interest in scientific community where mostly nanoclay and nanosilica [4], carbon nano-particle/fiber/tubes [5] and, polyhedral oligomeric silsesquioxane (POSS) [6], etc. have commonly been used. Though the thermal stability studies of TPU is widely reported, but for TPU–nanoclay composites they are yet to be fully explored. Some of the previous studies have shown that an optimum level of thermal stability can be achieved using 1–3% of modified nanoclay in the TPU-nanocomposites [7,8]. Reports on the use of montmorilonite (MMT), a natural layered silicate, have become common place [8]. However, laponite, the synthetic counter part of MMT, is relatively less popular in the published literature [8]. Owing to the hydrophobic nature of TPU, the clay platelets need to be surface modified to interact with the polymer such that the gallery spacing reaches to the stage of exfoliation [9]. In this context, surface modification of fillers by a surfactant (by single modification) has usually become the trend and also widely reported. However, scope of a dual modification sometimes can be more profitable but not explored [10]. Single modification is basically an ionic modification, whereas in the dual modification process the singly modified clay (by ion exchange) is further modified covalently by another surfactant.

In order to determine the thermal stability of polymeric materials, many model equations are routinely been used basically, which are differently modified or rearranged form of the basic Arrhenius equation which is based on the rate of degradation of the material and corresponding activation energy of the decomposition process. The determination of an activation energy parameter from a single integral TGA curve has been found to involve cumbersome curve-fitting techniques. Flynn and Wall's technique is a quick, simple method for determining activation energies directly from weight loss vs. temperature data at several heating rates [11]. On the other hand, Toop's equation can correlate life theory and TGA theory of a polymer. The equation is a shorter and more accurate alternative to the conventional expensive aging programs [12].

In this paper, we seek to derive a clearer picture of the effect of surface modification of various types of clay on the morphology, thermal, and thermo-dimensional stability over a range of temperature of the TPU–clay nanocomposites. Activation energies were evaluated from TGA data using well-known Flynn and Wall's technique [11]. Lifetimes of the nanocomposites, for the first time in reported literature, have been calculated using the

* Corresponding author. Tel.: +91 3222 281758; fax: +91 3222 282292.
E-mail address: santanuchat71@yahoo.com (S. Chattopadhyay).

0040-6031/$ – see front matter © 2010 Elsevier B.V. All rights reserved.
doi:10.1016/j.tca.2010.07.013

Toop's equation [12]. Dimensional stability has been measured by thermo-mechanical analyzer (TMA) over a useful temperature range suitable for applications of these nanocomposites for advanced systems.

2. Experimental

2.1. Materials used

A commercial grade of TPU (DP9380A), density 1110 kg/m^3 at 23 °C and hardness 82 Shore-A, was purchased from the Bayer Materials, Germany. The TPU was derived from polytetramethylene glycol (PTMEG) and diphenyl methane diisocyanate (MDI). Laponite RD® was supplied by the Southern clay limited, Mumbai, India and designated as 'L'. It is a disc-shaped synthetic hectorite magnesium silicate with diameter ~25 nm and mean thickness ~1 nm having empirical formula of $Na^{+0.7}[(Si_8Mg_{5.5}Li_{0.3})O_{20}(OH)_4]^{-0.7}$. Alumino-silicate based nanoclay (Cloisite 30B®, abbreviated as C30B) was obtained from Southern Clay Products, TX, USA. It contains organic quaternary ammonium ions $N^+(CH_2CH_2OH)_2CH_3)T$, where T represents an alkyl group with approximately 65% $C_{18}H_{37}$, 30% $C_{16}H_{33}$, and 5% $C_{14}H_{29}$. Nanomer I.30E-sodium MMT clay (NC, organically modified with octadecyl amine, mean dry particle size 8–10 μm, specific gravity 1.71, minimum mineral purity 98.5%) was procured from the Nanocor Corporation, USA. Octyltrimethoxysilane and 3-amino propyltriethoxysilane were purchased from the Sigma–Aldrich, USA and used for modification of laponite RD®. Cetyl trimethyl ammonium bromide (CTAB, designated as C) was obtained from the Merck Specialities Private Limited, India. Tetrahydrofuran (THF), analytical grade solvent for TPU, was purchased from the Qualigens, India.

2.2. Modification of clay

The inorganic laponite RD was modified with CTAB by using the standard ion exchange process [8]. The ionically modified laponite was designated as CL. 2 g of CL was dried in vacuum oven at 70 °C and was dispersed in 50 ml of dry toluene (dried over pressed sodium metal) in a two-necked round bottomed flask under nitrogen atmosphere. Thereafter, calculated amount of octyltrimethoxysilane was added, and the colloidal suspension was distilled for 6 h with continuous stirring. The solvent was dried, and excess amount of silane was extracted out with dry tolune by soxhletion for 12 h. The clay modified by this dual modified procedure was designated as COL. Similarly, when the ionically modified laponite (CL) was further modified with 3-amino propyltriethoxysilane, it was represented as CAPL.

2.3. Preparation of polyurethane–clay nanocomposites (PUCN)

8% solution of TPU was prepared in THF. 2 wt.% (with respect to TPU) of different modified laponites (e.g. CL, COL, and CAPL) and C30B and NC were separately mixed with THF and sonicated for 15 min. Thereafter, they were poured individually into separate TPU solutions and the stirring continued for 15 min followed by sonication for 15 min to make homogenous dispersions of different clays in TPU. Bubbles, if present in any dispersion, were removed by continuous stirring. The mixtures were then poured on a petridish covered with aluminium foil, evaporated to dryness at room temperature, and then kept in vacuum oven at 70 °C till constant weight. The samples were obtained in sheet form. In addition, pristine TPU sheet (without clay, designated as PUV) was also prepared, as above (control sample).

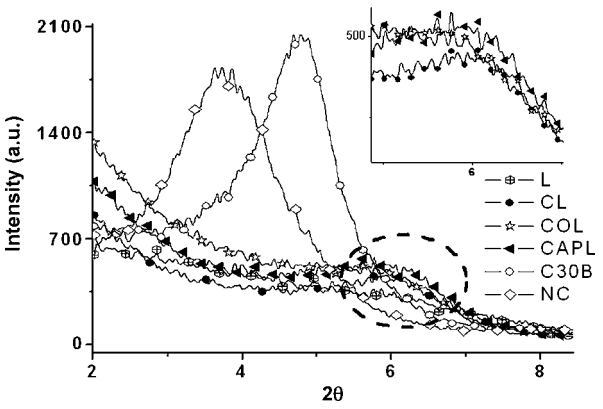

Fig. 1. WAXRD patterns at lower angular range for laponite (L) and modified organoclays (peaks for modified laponites are shown in the inset).

2.4. Characterization techniques adopted

X-ray diffraction (XRD) tests were conducted on the pristine as well as modified clay samples by a Philips Panalytical X-ray diffractometer (model: XPert Pro) using Cu target (Cu Kα) and Ni filter operating at a voltage of 40 kV and with a beam current of 30 mA. The wide angle XRD studies were done in the range of 2–10°. Fourier transformed infrared spectroscopy (FTIR) were conducted using modified clay filled KBR pallets in Nicolet Magna 550 FTIR spectrometer (Thermo Fisher Scientific, Madison, Wisconsin, USA, having resolution of 4 cm^{-1}). A JEOL JSM 5800 digital scanning electron microscope (SEM), Japan, was used to study phase morphology of various composites. The sample surfaces were sputter-coated with gold, and then examined by SEM at a tilt angle of 0° with an operating voltage of 20 kV. In order to understand the state of dispersion of the nanoclays in TPU, SEM fitted with energy dispersed X-ray analyzer (EDX, Oxford detector with dot mapping of Si, Mg or Al at 250×) was utilized. AFM analysis was performed by using Nanonics SPM1000 (Israel). Images of surface of completely dried films were recorded in air at room temperature using the tapping mode.

AFM photographs have been used for calculating the average roughness (R_a), root mean square roughness (RMS) and maximum height (R_{max}) which indirectly indicate the extent of filler dispersion. The dynamic mechanical analysis (DMA) was conducted using DMA 2980 of TA instruments Inc., USA, in tension mode with rectangular samples of dimensions 30 mm × (7–8) mm × (0.5–1) mm thickness. The rate of heating was 3 °C/min and the frequency was 1 Hz. TA Instruments Inc., USA, model TGA-2950 was used for the TGA measurements under argon atmosphere from room temperature to 600 °C at three different heating rates (e.g. 10, 20, and 30 °C/min) with sample weight 8–10 mg (approximately). Dimensional stability was determined by using thermo-mechanical analyzer (TMA-2940 of TA instruments, USA) where the samples were heated from −100 to 200 °C at a constant heating rate of 10 °C/min.

3. Results and discussion

3.1. Modification of clay

Evidences supportive of clay modification were ascertained by XRD, FTIR and TGA. From Fig. 1, it can be observed that the unmodified laponite (L) lacks of any specific well-defined peak within 2θ of 2–10°. However, in the cases of CL, COL and CAPL modification of filler generally imparts ordered diffractograms with formation of peaks between 5.5 and 6.5°. MMT based clays (e.g. C30B and NC), however, register their characteristic peaks at 4.7–4.8° and 3.6–3.9°, respectively.

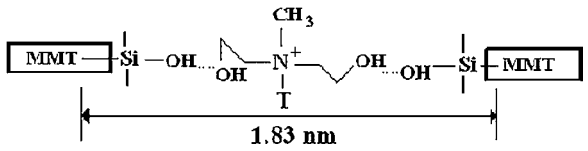

Scheme 1. Schematic representation of Cloisite 30B showing lesser spacing due to intense H-bonding.

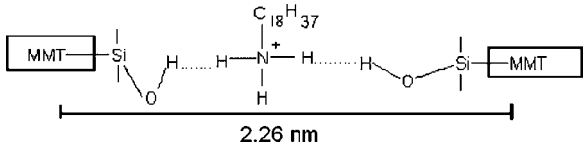

Scheme 2. Schematic representation of Nanomer I.30E showing increased gallery spacing owing to the weaker H-bonding.

C30B with stronger polar-polar (–OH) interactions between the clay gallery and surface modifying agent than that of NC, registers lower inter-gallery spacing (1.83 nm, approximately) compared to NC (2.26 nm). Similar observation in case of differently modified MMTs is reported in the literature [8,13]. Schematic representation of the –OH groups involved in polar-polar interactions are depicted in Schemes 1 and 2.

FTIR spectra as assigned in Table 1 give evidences of formation of new peaks corresponding to 1475 cm^{-1} ($C–H_{bend}$), 2850 cm^{-1} ($C–H_{str}$), and 2927 cm^{-1} ($C–H_{str}$) in case of CL as compared to unmodified laponite (L, devoid of any C–H bond) which confirm presence of duly modified surface by CTAB by cation exchange process [14]. Interestingly, the C–H stretching peaks of $>CH_2$ and $–CH_3$ groups (2850 and 2927 cm^{-1}) were observed in case of both COL and CAPL. The presence of the peaks, in case of both COL and CAPL, at 3428 cm^{-1} ($O–H_{str}$), 1655 cm^{-1} ($O–H_{bend}$) and 540 cm^{-1} ($Si–O–Si_{bend}$) (Table 1, Scheme 3) were also observed. The addition of an extra peak corresponding to $N–H_{bend}$ at 1563 cm^{-1} is noted in case of CAPL only. Of course, the signals corresponding to O–H group (both stretching and bending) might be due to presence of either of the absorbed water or O–H bond present in the pristine laponite itself. Summary of FTIR observations confirms appropriate ionic and covalent modifications of laponite.

Table 1
FTIR band frequencies of various modified laponites.

Sample ID	Band frequency (cm^{-1})	Assigned bond
CL	1475	$C–H_{bend}$
	2850	$C–H_{str}$
	2927	$C–H_{str}$
COL	540	$Si–O–Si_{bend}$
	3428	$O–H_{str}$
	1655	$O–H_{bend}$
	2850	$C–H_{str}$
	2927	$C–H_{str}$
CAPL	540	$Si–O–Si_{bend}$
	3428	$O–H_{str}$
	1655	$O–H_{bend}$
	1563	$N–H_{bend}$
	2850	$C–H_{str}$
	2927	$C–H_{str}$

TGA thermograms of the modified (single/dual) clay show thermal degradation to the extent of 14.5, 21.0, and 21.0%, respectively, for CL, COL, and CAPL in between 200 and 600 °C as compared to pristine laponite (L, with a negligible amount of degradation). TGA results, giving higher thermal degradation values for organically modified versions of laponite [15] are, therefore, supportive of XRD and FTIR findings.

3.2. Characterization of TPU–clay nanocomposites

SEM photomicrographs (Fig. 2) and their respective EDX dot maps (Fig. 3) exhibit the nature of dispersion as well as the size of the dispersed particles in the matrix. The brighter features in the figures represent the clay aggregates. The EDX dot maps further confirm the presence of Si on the rough bloomed surface. All the modified montmorillonite based nanocomposites like PUC30B (Fig. 2a) and PUNC (Fig. 2b) show uniform clay dispersion into the matrix. Attainment of optimum amount of the polar surfactant through dual surface modification onto surface of organo-clay resulted in better dispersion of the filler particles into the TPU matrix. As a result, dual modified composites PUCAPL (Fig. 2c) and PUCOL (Fig. 2d) show better filler dispersion than PUCL (Fig. 2f). As expected, the absence of filler in neat PU generates a smooth surface (Fig. 2e) contrary to nanocomposites.

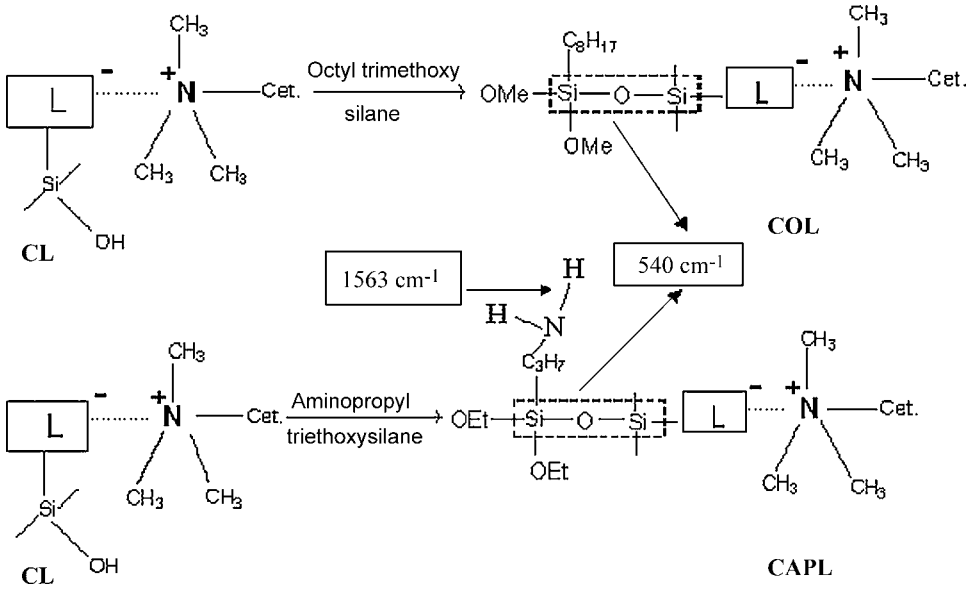

Scheme 3. Covalent bond formation due to silylation of surfactant modified laponite clay and their characteristic IR frequency.

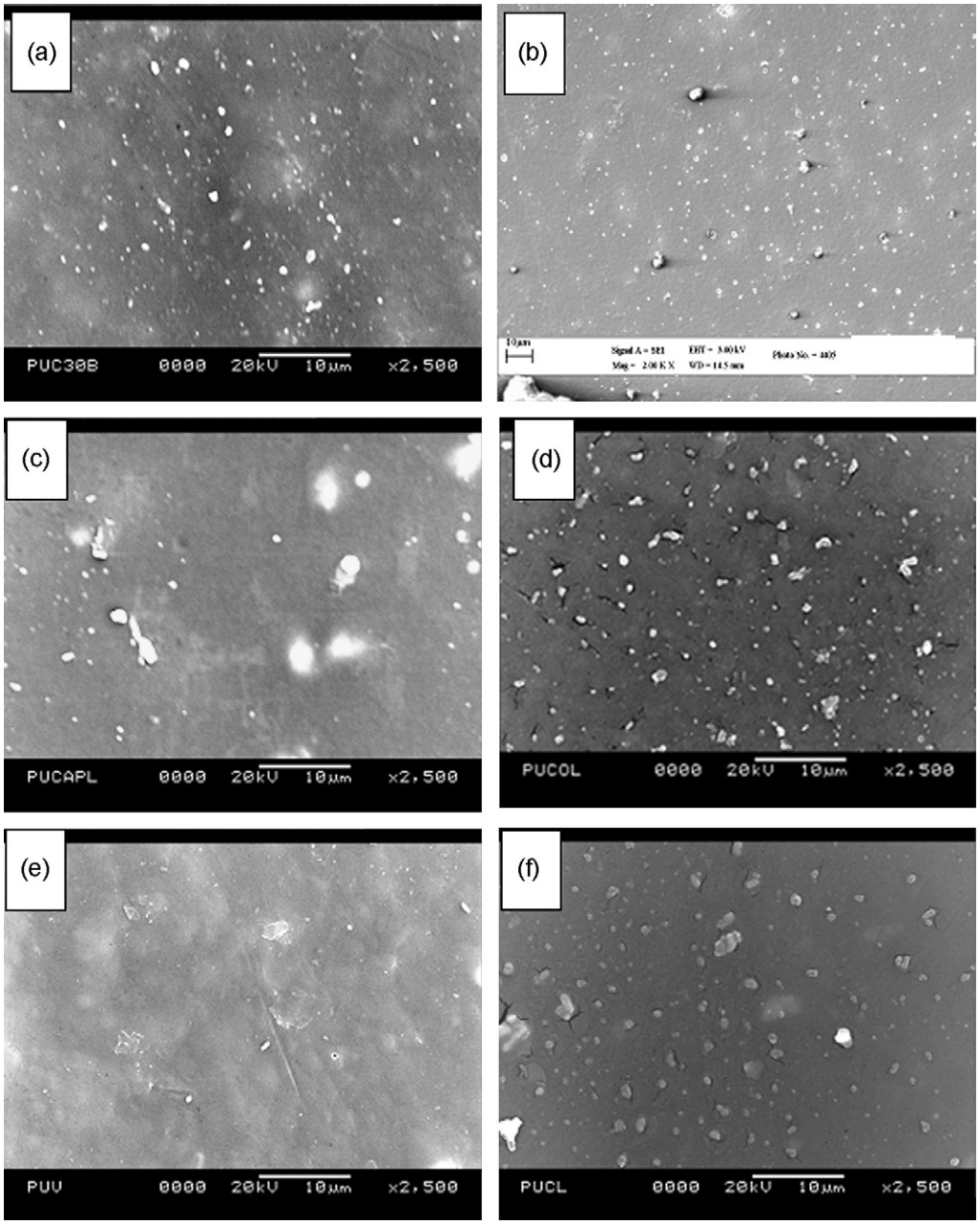

Fig. 2. SEM photomicrographs (2500× magnification) of different nanocomposites: (a) PUC30B, (b) PUNC, (c) PUCAPL, (d) PUCOL, (e) PUV and (f) PUCL.

AFM 3D topography images of surface of different nanocomposites are shown in Fig. 4a–f. Calculated values of average roughness (R_a), root mean square roughness (RMS) and maximum height (R_{max}) are given in Table 2. The surface roughness can be increased either by formation of excess of clay agglomeration or due to surface shrinkage on evaporation of solvent during nanocomposite preparation [16]. The AFM analysis on montmorillonite clay composites showing lower roughness supports our SEM observation

Table 2
Average roughness (R_a), root mean square roughness (RMS), and maximum height roughness (R_{max}) values of polyurethane–clay nanocomposite.

Sample ID	Average roughness (R_a) value[a] (μm)	Root mean square roughness (RMS) value[a] (μm)	Maximum height roughness (R_{max}) value[a] (μm)
PUV	0.050	0.059	0.407
PUCL	0.017	0.021	0.107
PUCOL	0.083	0.093	0.539
PUCAPL	0.068	0.124	2.230
PUC30B	0.012	0.014	0.082
PUNC	0.016	0.023	0.173

[a] Maximum error percentage is limited to ±3%.

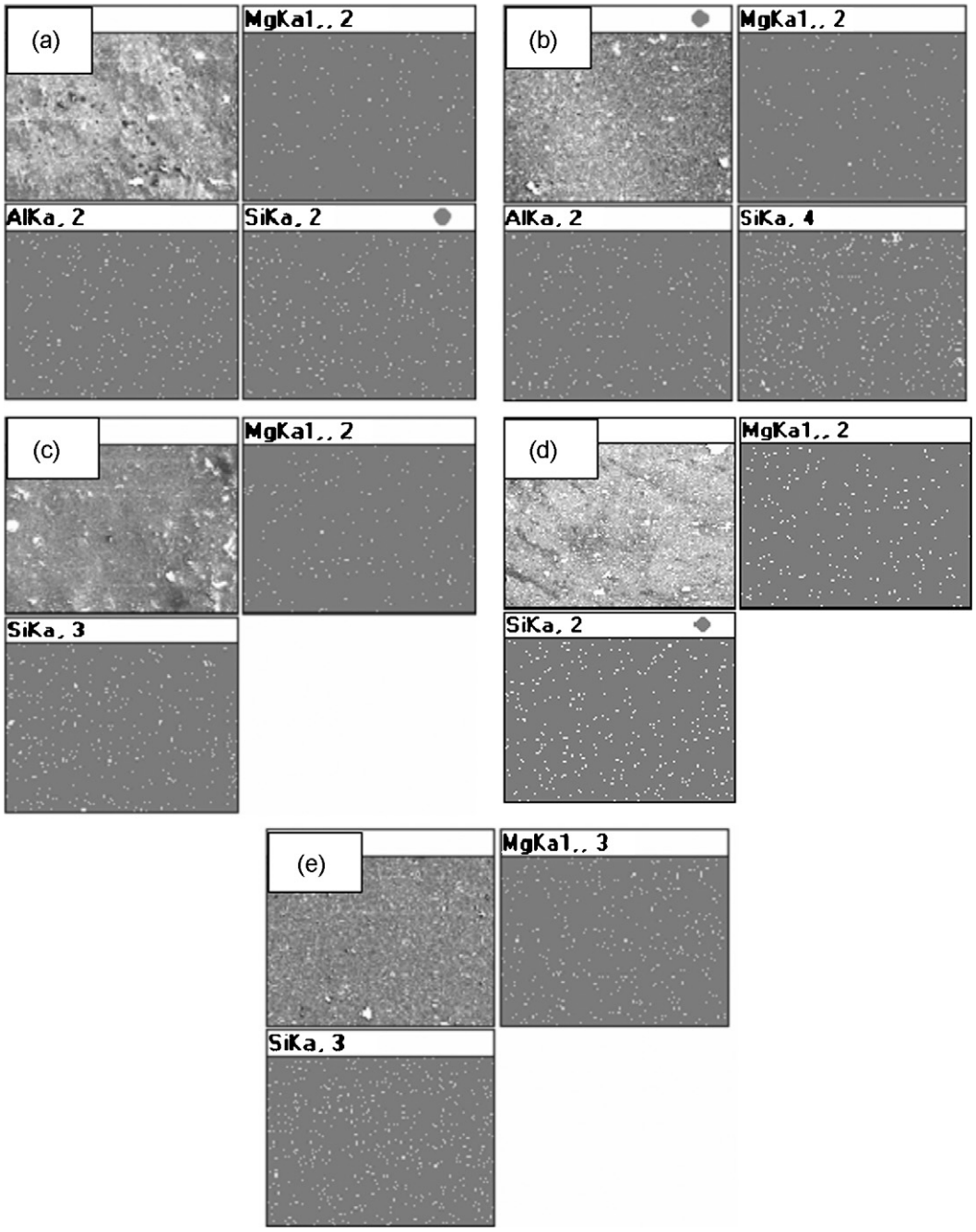

Fig. 3. EDX dot maps (250× magnification) of different nanocomposites: (a) PUC30B, (b) PUNC, (c) PUCAPL, (d) PUCOL and (e) PUCL, for each set first one represents the topography and other ones are respective dot maps.

[compare Table 2 and SEM photomicrographs (Fig. 2a and b)]. Literature on preparation of nanocomposites by solvent evaporation technique described the cause of reduced roughness to be the effect of restrained mobilization of polymer chains in presence of MMT [16].

Storage modulus, loss modulus and tan delta plots, obtained from the DMA experiments, have been shown in Fig. 5a–c, respectively. For all the samples, storage modulus decreases with temperature and approaches to more or less similar values near to glass transition temperatures (T_g, ranging between −20 and −40 °C, as observed from Fig. 5c). In case of singly modified laponite (PUCL and PUCOL), the storage moduli below T_g were found to be more than neat PUV. However, commercial montmorilonite (PUC30B and PUNC) based composites and dual modified laponite PUCAPL show similar trend of nearly overlapping values of storage modulus throughout the entire temperature region. This is possibly the manifestation of better polymer–filler interaction in PUCAPL prepared by dual filler modification which brings its performance closer to commercially available montmorillonites.

The loss moduli of the composites in Fig. 5b, according to their peak maxima, can be arranged in the order PUNC < PUCAPL < PUC30B < PUV < PUCOL < PUCL which follows exactly the trend according to the discussions made above. It can, therefore, be predicted that the viscoelastic properties of PUCAPL is comparable to commercial montmorillonites based nanocomposites (PUNC and PUC30B), and dual modification of laponite is more effective than single modification (e.g. in case of PUCOL and PUCL). The shifting of T_g towards more negative temperature

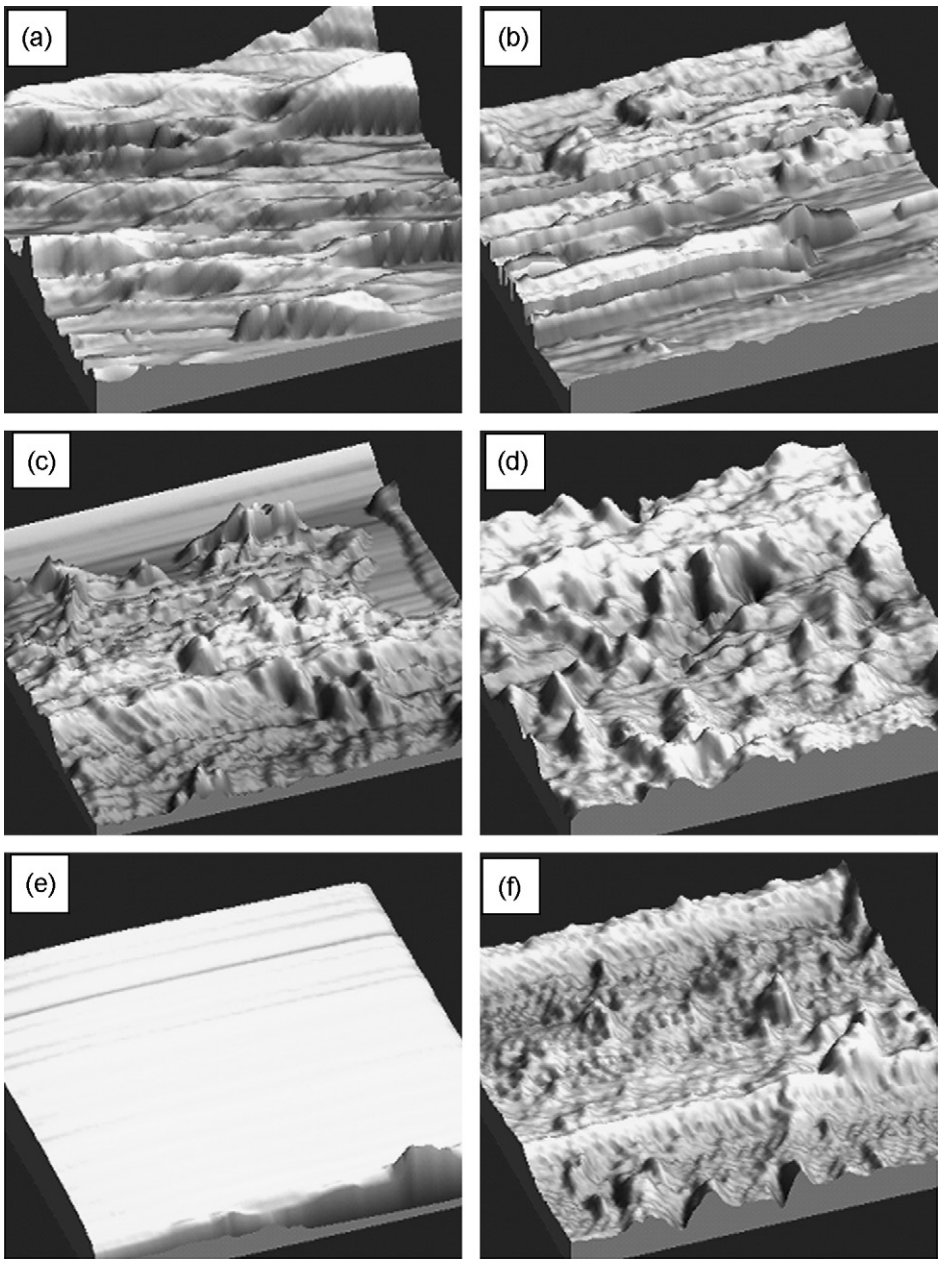

Fig. 4. AFM 3D topographs (scan area:1 μm × 1 μm) of different nanocomposites: (a) PUV, (b) PUCL, (c) PUCOL, (d) PUCAPL, (e) PUC30B and (f) PUNC.

side in the tan delta plot in Fig. 5c possibly indicate a 'thin film effect' [13] due to coverage of surfaces of clay platelets by polymer chains which again is proportional to the extent of polymer–filler interaction. This, in effect, resulted in better dynamic properties of PUCAPL, PUNC and PUC30B.

TMA thermograms of the composites are shown in Fig. 6, and the derivative TMA results are summarized in Table 3. Maximum rate of expansion and contraction values for the PUCAPL are in between those of PUNC and neat PUV. The enhanced polymer–filler interaction in case of PUCAPL similar to PUNC, as has been observed in case of DMA studies, can be correlated with flexibility and higher expansion and contraction values. In general, it is observed that the higher aspect ratio of the clay, presence of alkyl/alkoxy side chains, and polarity incorporated by surface medication of clay influence the mobility of the polymer chains which in turn affect the relative viscoelasticity and dimensional changes of the composites. Maximum rate of expansion and contraction for PUCL and PUCOL are, therefore, lower than those of PUCAPL, PUNC and PUV.

However, Cloisite 30B shows values of expansion/contraction similar to PUCL and PUCOL rather than PUNC or PUCAPL. The apparently anomalous result can be substantiated by the AFM result on reduced roughness of the composite in presence of filler (Table 2) owing to restriction caused by the filler particles against chain slippage during solvent evaporation at the time of sample preparation for AFM. SEM photomicrograph for PUCL shows presence of many clay aggregates (Fig. 2f) which eventually increased restriction for the polymer chains in slipping past on the filler surface and demonstrate higher shrinkage during AFM sample preparation. The extent of contraction grows to the level to match values of PUCAPL or PUNC.

The TGA and DTG thermograms (Fig. 7a and b) of all the PUCNs show that the nanocomposites including PUV are reasonably stable up to 250 °C. In fact, the first stage of decomposition of pristine TPU starts at the earliest and is mainly dominated by the scission of hard segment, while the second step corresponds to decomposition of the soft segment (Table 4) [8]. PUC30B and PUNC show com-

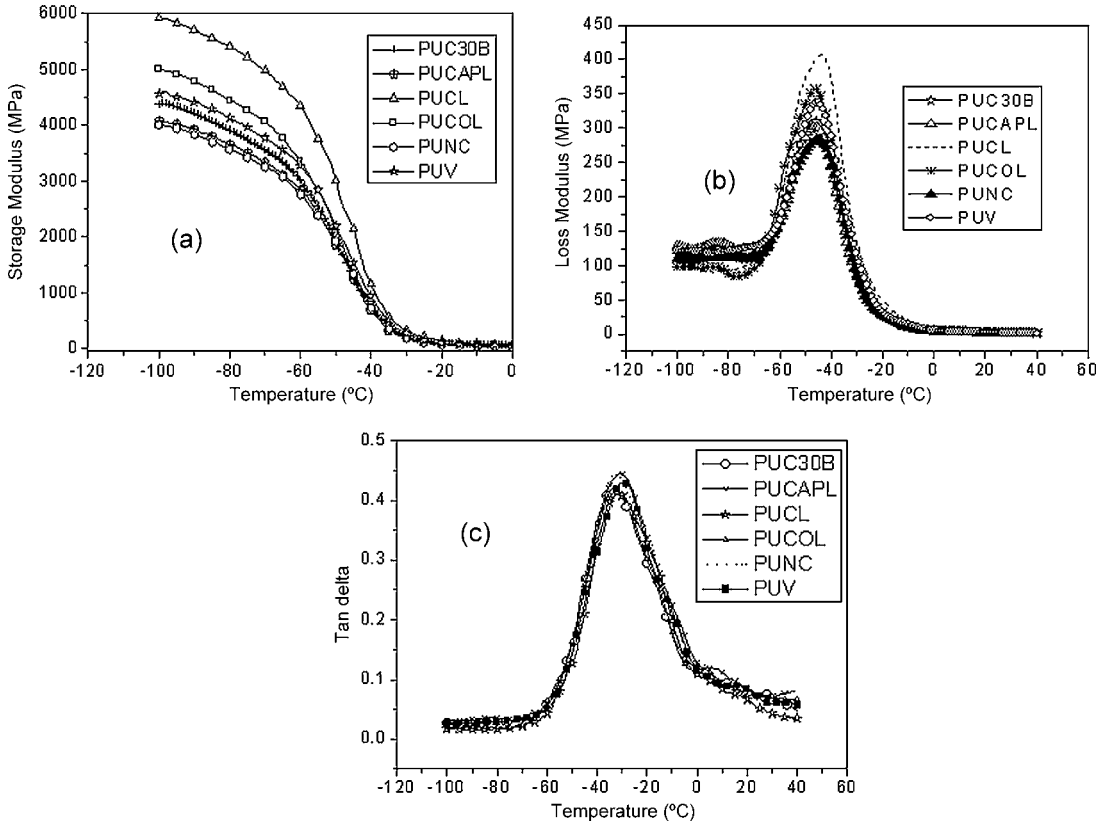

Fig. 5. DMA temperature sweep results (a) storage modulus vs. temperature (up to 0 °C is shown here), (b) loss modulus vs. temperature, (c) tan delta vs. temperature.

Table 3
Volume expansion and contraction data from the TMA thermograms.

Sample ID	Expansion (%)[a]	Max. rate of expansion (μm/min)[a]	Contraction (%)[a]	Max. rate of contraction (μm/min)[a]
PUV	7.3	6.9	29.7	48.6
PUCL	4.4	3.0	16.7	9.7
PUCOL	2.1	2.1	17.9	12.4
PUCAPL	6.7	6.0	25.7	37.8
PUC30B	0.9	1.5	9.6	12.2
PUNC	2.1	5.4	15.7	25.3

[a] Maximum error percentage is limited to ±4%.

parable thermal stability. However, the ultimate residue of 8.2% at 600 °C in case of PUC30B is more than PUNC. This is possible by formation of stable ether linkages due to interaction between the two adjacent –OH groups in case of PUC30B. Greater thermal stability for these types of modified clays has also been reported by Wang et al. due to strong covalent bond formation (C–O and N–C) between the urethane linkages and the modified montmorillonites [17]. Interestingly, PUCAPL shows comparable thermal stability reflected by PUC30B and PUNC for their first step decomposition. However, better polymer–filler interaction and due to thin film effect, as discussed earlier, caused higher thermal stability of PUCAPL as compared to MMT based nanocomposites. This is reflected with reduced weight loss of 36.9% as well as a higher residual content of 9.1% at 600 °C for PUCAPL than PUNC or PUC30B. Possibly polar functionality ($-NH_2$) of CAPL interacts with TPU matrix and forms comparatively strong carbamide bond eventually forming higher amount of residue as per Scheme 4. Similar type of carbamate–amine reaction has been reported by Uno et

Table 4
Decomposition temperature and % residue of PUCN from TGA.

Sample	First step of decomposition		Second step of decomposition		Residue at 600 °C (%)[a]
	Onset temp. (°C)[a]	Weight loss (%)[a]	Onset temp. (°C)[a]	Weight loss (%)[a]	
PUV	289.5	43.9	407.7	48.3	7.7
PUCL	292.8	45.0	394.8	47.8	5.9
PUCOL	295.6	46.4	394.6	46.3	6.5
PUCAPL	308.7	52.9	415.4	36.9	9.1
PUC30B	320.3	46.9	416.6	45.0	8.2
PUNC	311.7	47.0	420.7	48.6	4.7

[a] Maximum error percentage is limited to ±1%.

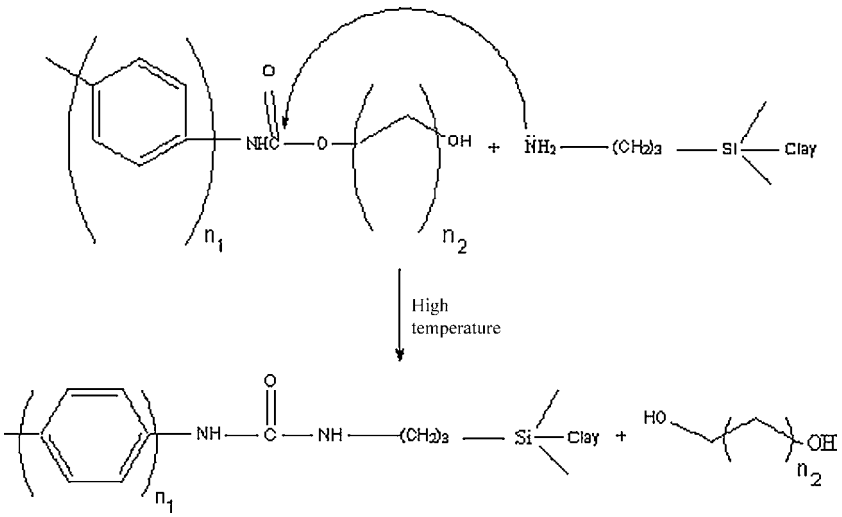

Scheme 4. Possible decomposition pathway for PU reacting with polar functionality of clay.

al. [18]. Other modified laponite based nanocomposites, e.g. PUCL and PUCOL show less thermal stabilities than PUCAPL, PUC30B or PUNC.

3.3. Kinetics of thermal decomposition by multiple heating rate method

Kinetic results, calculated using Flynn–Wall technique (Eq. (1) in Appendix), have been summarized in Table 5. All the kinetic parameters are computed using the software Universal V4.2E provided by TA instruments, USA. The results show that similar activation energies (E) are required for decomposition of PUCAPL, and PUC30B, while it is marginally higher in the case of PUCL and PUCOL. But PUNC always shows considerably higher activation energies. Beyond 20% conversion, values of E become similar for PUV, PUCOL and PUCL, as by then all the surface modifiers must have been degraded to attain the required stage of decomposition. It can also be observed that at 20% percent conversion and higher, necessitates a higher level of activation energy for PUV, PUCL and PUCOL. On the contrary, for PUCAPL, PUC30B and PUNC, as the percentage conversion is increased, the activation energy level decreases initially up to 20% conversion level, and thereafter they are increased with increasing conversion level. As activation energy is not constant for various extent of conversion, it can be inferred that the thermal degradation of these nanocomposites follows a complicated rate process. For the samples PUCOL, PUNC having nonpolar modified clay, requirement of activation energy is higher at higher conversion levels. At higher temperature, nanocomposite having clay with polar (–OH, $–NH_2$, etc.) modification gives rise to ran-

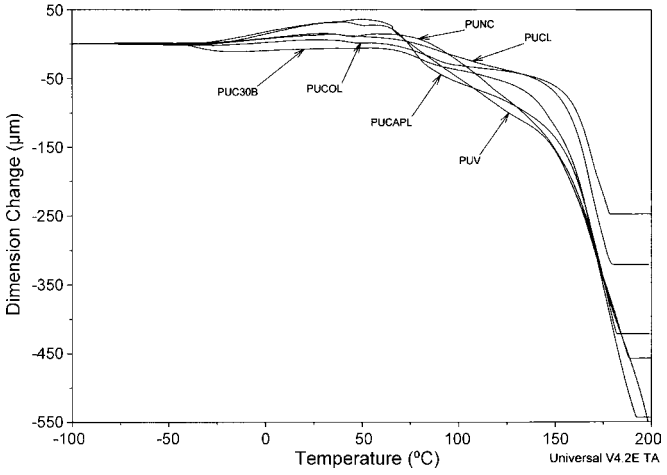

Fig. 6. TMA thermograms of the polyurethane–clay nanocomposites and virgin polyurethane (PUV) at a heating rate of 10 °C/min.

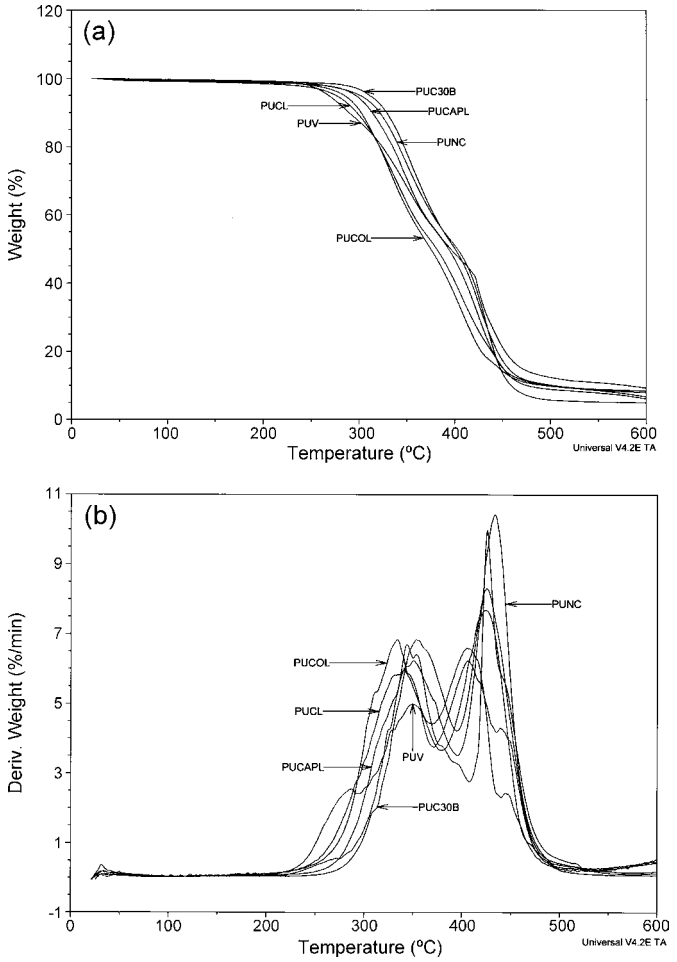

Fig. 7. (a) TGA thermograms of the polyurethane–clay nanocomposites and virgin polyurethane (PUV) at a heating rate of 10 °C/min. (b) DTG thermograms of the polyurethane–clay nanocomposites and virgin polyurethane (PUV) at a heating rate of 10 °C/min.

Table 5
Kinetic results calculated using Flynn–Wall technique.

Conversion (%)	Activation energy, E^a (kJ/mol)					
	PUV	PUCL	PUCOL	PUCAPL	PUC30B	PUNC
5	61.5	98.4	92.5	91.7	92.6	159.5
10	63.7	101.5	97.0	89.6	89.7	140.6
15	71.6	101.0	102.2	88.9	87.3	136.4
20	85.6	102.8	108.3	91.2	87.4	138.3
25	100.8	106.6	115.9	94.2	89.1	141.0
30	112.0	112.6	121.9	97.7	90.7	146.3
35	120.8	120.3	127.8	99.0	95.3	153.0
40	132.5	129.6	133.8	101.1	102.1	162.2

[a] Maximum error percentage is limited to ±2%.

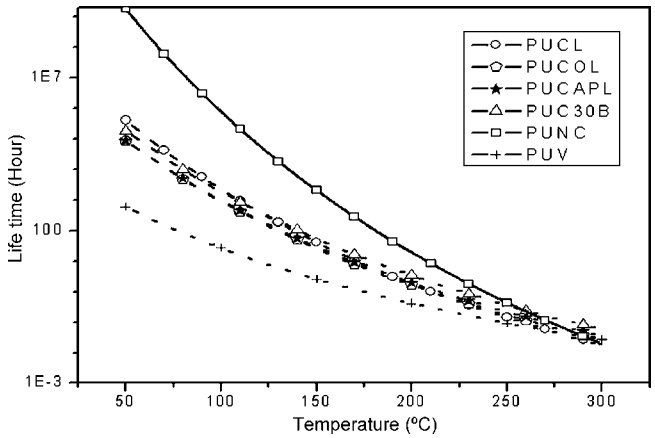

Fig. 8. Variation of lifetime with temperature of PUCNs taking kinetic parameters at conversion level of 5%.

dom scission of the urethane linkages (possible reaction for $-NH_2$ is shown in Scheme 4) and thus the degradation rate of the polymer backbone is enhanced. The lack of polar group in PUCL imparts higher '*E*' than the composites having clays with polar modifications (PUCAPL, PUC30B).

3.4. Estimation of lifetime

The lifetime of the nanocomposites has been determined using the Toop's equation [9,10] (Eq. (2) in Appendix). Lifetime is temperature dependent and decreases exponentially with increase in temperatures (Fig. 8). In accordance with the TGA results, higher lifetimes have been obtained for the MMT based nanocomposites. Interestingly, at the lower temperature ranges (between 50 and 200 °C), among modified laponite based nanocomposites, PUCL (singly modified one) shows the higher stability than the other dual modified laponite based composites (PUCAPL and PUCOL). Of course, at the higher temperature ranges (200–300 °C), PUCAPL and PUCOL regains superiority over PUCL. Moreover, between 255 and 275 °C, the order of the estimated lifetime for various nanocomposites follows the order: PUC30B > PUNC > PUCAPL > PUCOL > PUCL > PUV. This order is identical to the order of degradation onset temperature found in Table 4. Also interesting is to note that the dispersion characteristics of the particulate phases in the SEM photomicrographs (Fig. 2) correlate well with lifetime estimations.

4. Conclusions

1. An attempt has been made to explore the possibility of evolving substitute of montmorillonite based clays which are effective for development of polymer–clay nanocomposites.
2. Laponites which are commercially available in a more pure form and structurally similar to MMT has been considered as a potential additive.
3. Dual surface modification of laponite has been found to be sometimes more effective/equivalent to Cloisite in terms of thermal, thermo-dimensional and lifetime expectation of nanocomposites composed of MMT.
4. Incidentally, laponites show same effectivity at equal filler concentration, e.g. at similar wt.% of MMT used for nanocomposites fabrication.
5. Thermal stability, lifetime, activation energies of the clay filled polyurethane nanocomposites are largely dependent on the aspect ratio, polarity and the types of filler surface modification (ionic/covalent by single or dual steps).

Appendix A. Theory

A.1. Flynn and Wall's technique

It is used to calculate the activation energy based on the Arrhenius equation employing multiple heating rates in TGA and the relevant expression is,

$$\ln q = \ln(ZE/R) - \ln(\alpha) - 0.4567\,E/RT \quad (1)$$

where E is calculated from the slope of a plot of $\ln q$ vs. $1/T$ for a constant α, which is equal to $(-E/R)$, and $\ln(Z)$ is the frequency factor.

A.2. Toop's equation

The lifetime of the nanocomposites has been determined using the following equation recommended by Toop,

$$\ln t_f = (E/RT_f) + \ln[E/qR\,P(X_f)] \quad (2)$$

where t_f is the estimated time of failure (in min); T_f is the failure temperature (K); $P(X_f)$ is the function and its value depends on E at the failure temperature (K).

References

[1] T. Gupta, B. Adhikari, Thermochim. Acta 402 (2003) 169–181.
[2] A. Lendlein, S. Kelch, Angew. Chem. Int. Ed. 41 (2002) 2034–2057.
[3] A. Lendlein, R. Langer, Science 296 (2002) 1673–1676.
[4] I.V. Khudyakov, R.D. Zopf, N.J. Turro, Des. Monomers Polym. 12 (2009) 279–290.
[5] J. Ryszkowska, M.J. Kowalska, T. Szymborski, K.J. Kurzydlowski, Physica E 39 (2007) 124–127.
[6] B.X. Fu, B.S. Hsiao, H. White, M. Rafailovich, P.T. Mather, H.G. Jeon, S. Phillips, J. Lichtenhan, J. Schwab, Polym. Int. 49 (2000) 437–440.
[7] F. Cao, S.C. Jana, Polymer 48 (2007) 3790–3800.
[8] A.K. Mishra, G.B. Nando, S. Chattopadhyay, J. Polym. Sci. Part B: Polym. Phys. 46 (2008) 2341–2354.
[9] A. Leszczyĩnska, J. Njuguna, K. Pielichowski, J.R. Banerjee, Thermochim. Acta 453 (2007) 75–96.
[10] J. Wang, P.A. Wheeler, W.L. Jarrett, L.J. Mathias, J. Appl. Polym. Sci. 106 (2007) 1496–1506.

[11] J.H. Flynn, L.A. Wall, J. Polym. Sci. Part B: Polym. Lett. 4 (1966) 323–328.
[12] P. Paik, K.K. Kar, Polym. Degrad. Stab. 93 (2008) 24–35.
[13] S. Praveen, P.K. Chattopadhyay, P. Albert, V.G. Dalvi, B.C. Chakraborty, S. Chattopadhyay, Composites: Part A 40 (2009) 309–316.
[14] N.N. Herrera, J.L. Putaux, E.B. Lami, Prog. Solid State Chem. 34 (2006) 121–137.
[15] N.N. Herrera, J.M. Letoffe, J.L. Putaux, L. David, E.B. Lami, Langmuir 20 (2004) 1564–1571.
[16] H.C. Kuan, C.M. Ma, W.P. Chuang, H.Y. Su, J. Polym. Sci. Part B: Polym. Phys. 43 (2005) 1–12.
[17] C.H. Wang, Y.T. Shieh, S. Nutt, J. Appl. Polym. Sci. 114 (2009) 1025–1032.
[18] K. Uno, K. Niume, T. Nakayama, Y. Iwakura, Polym. J. 6 (1974) 348–355.